Title: Unveiling lipid chemodiversity in root exudates: A comprehensive characterization of the exudate metabo-lipidome in a perennial grass

Sneha P. Couvillion[1] (0000-0003-0307-9343), Isabella H. Yang[1] (0000-0002-1490-3329), Dylan Hermosillo[1] (0009-0007-8638-148X), Josie Eder[1] (0000-0002-2876-0496), Sheryl Bell[1] (0000-0001-8445-1375), Kirsten S. Hofmockel[1,*] (0000-0003-1586-2167)

[1]Earth and Biological Sciences Directorate, Pacific Northwest National Laboratory, Richland, WA, USA

*Corresponding author: kirsten.hofmockel@pnnl.gov

Keywords: metabo-lipidomics, root exudates, lipids, mass-spectrometry, tall wheatgrass, metabolite annotation, rhizodeposition, molecular chemodiversity

Abstract

The rhizosphere, where plant roots meet soil, is a hub of biogeochemical activity with ecosystem impacts on carbon stocks. Root derived carbon has been found to contribute more to soil carbon stocks than aboveground litter. Nonetheless, the molecular chemodiversity of root exudates remains poorly understood due to limited characterization and annotation. Here our goal was to discover the molecular chemodiversity of metabolites and lipids in root exudates to advance our understanding of plant root inputs belowground. We worked with mature, field-grown tall wheatgrass (*Thinopyrum ponticum*) and optimized exudate collection protocols to enable the capture of non-polar lipids in addition to polar and semi-polar metabolites. Rates of carbon input via hydrophobic exudates were approximately double that of aqueous exudates and carbon/nitrogen ratios were markedly higher in hydrophobic compared to aqueous exudates, emphasizing the importance of lipids, due to their high carbon content. To maximize molecular coverage of exudate chemodiversity, we used liquid chromatography coupled tandem mass-spectrometry for paired untargeted metabolomics and lipidomics or 'metabo-lipidomics'. We substantially increased the characterization of exudate chemodiversity by employing both

tandem mass spectral library searching and deep learning-based chemical class assignment. Notably, in this unprecedented characterization of intact lipids in root exudates, we discovered a diverse variety of lipids, including substantial levels of triacylglycerols (~19 µg/g fresh root per min), fatty acyls, sphingolipids, sterol lipids, and glycerophospholipids. Comparison of the root exudate and tissue lipidomes revealed minimum glycerophospholipids in exudates, suggesting the exudate protocol did not extract lipids from root cell membranes.

Introduction

Root Exudates: Major Carbon Inputs and Regulators of Soil Organic Matter (SOM) Dynamics

Current estimates of direct plant contributions to SOM pools such as mineral associated organic matter (MAOM) are likely undervalued given the reliance on aboveground plant tissue proxies for determining plant versus microbial origin (Whalen *et al.*, 2022). This is in part due to the challenging nature of quantifying rates, chemical composition and ecological significance of root derived rhizodeposits including exudates (Phillips *et al.*, 2008). The roles of small molecule metabolites, especially lipids, in shaping interkingdom interactions and microbial processes that control cycling and long-term storage of carbon are poorly understood. Metabolites and lipids play diverse roles in regulatory, metabolic, and signaling networks among microbes (Whiteley *et al.*, 2017, Khalid & Keller, 2021) and in microbe-plant interactions (Chagas *et al.*, 2018) and are sensitive indicators of organismal phenotypes and community metaphenomes (Jansson & Hofmockel, 2018). However, challenges in identifying key molecules and interpreting their functions are critical frontiers in soil ecosystem research (Brown *et al.*, 2024).

Plants carry out the necessary first step of siphoning atmospheric carbon into soil through photosynthesis. It is estimated that 5-40% of photosynthetically fixed carbon enters soil through root exudation (Simon & Haichar, 2019, BADRI & VIVANCO, 2009). Exudates regulate SOM dynamics by contributing to SOM stabilization and turnover. Small molecules in root exudates, such as lipids, function as both signaling compounds and microbial nutrients that shape the assembly and activity of microbial communities (Huang *et al.*, 2019, Zhalnina *et al.*, 2018, Mark

59 *et al.*, 2005, Hugoni *et al.*, 2018, Sasse *et al.*, 2018). They influence the colonization, growth, and
60 activity of key microbial members, including mycorrhizal fungi (Tian *et al.*, 2021, Elias & Safir,
61 1987), impact soil physical structure (Naveed *et al.*, 2017), induce soil respiration (de Vries *et al.*,
62 2019), and can cause priming, decomposition, and mineralization of SOM. These small molecules
63 may regulate microbial metabolism, undergo assimilation into microbial biomass, transformation
64 by extracellular enzymes, or association with soil minerals, ultimately integrating into SOM.
65 Research on priming (Fontaine *et al.*, 2007, Chen *et al.*, 2019) and factors controlling the
66 formation of stable SOM (Liang *et al.*, 2023, Kallenbach *et al.*, 2016, Rempfert *et al.*, 2024) have
67 predominantly used single or simplistic plant carbon input surrogates such as glucose, cellulose
68 and cellobiose. However, this approach overlooks the realistic chemodiversity present in
69 exudates. By relying on these surrogates, the studies tend to simplify plant inputs to carbon
70 sources alone, neglecting the diverse metabolic, regulatory, and signaling roles played by the
71 small molecules present in exudates. Different chemical classes of root exudate surrogates induce
72 distinctly different magnitudes of priming and these effects are likely non-additive in complex
73 mixtures, emphasizing the complexity of their effects on SOM stocks (Yan *et al.*, 2023) and the
74 need to consider root exudate molecular complexity.
75
76 **Capturing Exudate Chemodiversity using Metabo-Lipidomics: Navigating Beyond just Sugars**
77 **and Organic Acids into the Uncharted Territory of Lipids**
78 Recent studies using liquid chromatography coupled with mass spectrometry (LC-MS/MS) for
79 untargeted metabolomics have revealed a broad spectrum of polar and semi-polar small
80 molecules in exudates (McLaughlin *et al.*, 2023, Dietz *et al.*, 2019). While progress has been
81 achieved in characterizing these metabolites, the comprehensive identification of the numerous
82 features detected by mass spectrometry remains a significant bottleneck in metabolomics, with
83 only a small fraction of features being currently identified (da Silva *et al.*, 2015, Giera *et al.*, 2022,
84 Shen *et al.*, 2023). Importantly, the exploration of lipids, a crucial group of non-polar metabolites,
85 is notably absent in root exudate studies. Their distinctive hydrophobic properties present
86 challenges in detection and analysis using conventional methods for exudate collection and
87 analysis. Our recent work demonstrates the value of intact lipids in soil ecosystems as sensitive

indicators of environmental stress response and substrate availability and highlights their great potential for interrogating interkingdom interactions and resource sharing (Couvillion *et al.*, 2023, Naasko *et al.*, 2023).

In this study, we hypothesized that plant roots exude a diverse array of intact lipids, potentially serving as microbial energy sources, chemotactic signals, antimicrobial compounds, and metabolic regulators in the rhizosphere. Accurately assessing plant exudate profiles, which are significantly influenced by growth stage and growth conditions, requires collecting root exudates from mature plants in a way that realistically recapitulates natural field conditions (Dietz et al., 2019, Williams *et al.*, 2021). This was highlighted by a recent study which found higher total carbon in hydroponic exudates, whereas field-grown plant exudates contained more secondary metabolites- suggesting hydroponic root exudates may not fully capture the exudate composition and chemodiversity of field environments (Heuermann *et al.*, 2023). We chose to work with mature, field grown tall wheatgrass plants (*Thinopyrum ponticum*, cultivar: Alkar) to maximize translation to perennial plants in the field. To collect the full diversity of small molecules, we optimized exudate collection protocols to enable the capture of non-polar (hydrophobic) lipids in addition to polar and semi-polar (hydrophilic) metabolites. We found that C and N input rates in hydrophilic and hydrophobic exudates were 38.41 $\pm$ 5.93 and 81.52 $\pm$ 13.81 μg C g^{-1} fresh root mass min^{-1}, respectively, and 2.68$\pm$ 0.42 and 0.20 $\pm$ .04 μg N g^{-1} fresh root mass min^{-1}, respectively (**Fig. 1**). The C/N of hydrophilic exudates was far lower than that of hydrophobic exudates (14.40 $\pm$ 0.58 vs 459 $\pm$ 90), which is consistent with high C content in lipids, and points to potential differences in metabolite and lipid contributions to SOM dynamics. To explore the molecular diversity of root

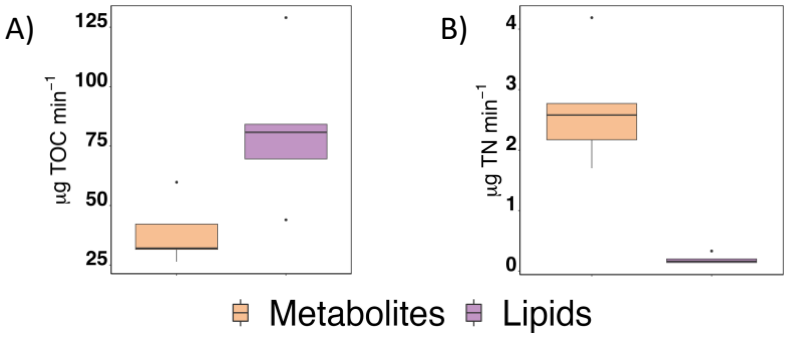

Figure 1: A) Total organic carbon (TOC) and B) total nitrogen (TN) input rates in aqueous metabolite (orange) and hydrophobic lipid (lilac) root exudate fractions, normalized to root mass

exudates, We used liquid chromatography coupled tandem mass-spectrometry (LC-MS/MS) for paired untargeted metabolomics and lipidomics or 'metabo-lipidomics' (**Fig. 2A**); we employed three liquid chromatography column chemistries and analyzed samples in positive and negative ionization modes to maximize coverage of the metabo-lipidome. The results from the metabolomics and lipidomics analyses will be discussed separately.

Tackling the Unknowns: Enhancing Metabolite Annotation and Classification by Combining Spectral Library Searching with CANOPUS

Metabolite identification in mass-spectrometry analyses poses a major challenge in metabolomics research (Monge *et al.*, 2019). To address this, our study combines two strategies for improved feature annotation. We employed spectral library searching (SLS) to assign annotations to 224 unique metabolites (Schymanski confidence level 2A (Schymanski *et al.*, 2014), **Fig 2B**), using in-house and publicly available MS/MS databases. These annotations were established through accurate mass and tandem mass spectra matching, with additional consideration of retention time when there was a match to the in-house library. Using the SLS approach we identified 67 metabolites belonging to the 'Organic acids and derivatives' superclass, primarily comprising amino acids and analogues, and dipeptides. The 'Lipids and lipid-like molecules' superclass ranked second, encompassing 44 metabolites, predominantly composed of fatty acids, derivatives, and prenol lipids. The 'Phenylpropanoids and polyketides' superclass contained 30 metabolites, including cinnamic acids and derivatives, flavonoids, coumarins, phenylpropanoic acids, and cinnamaldehydes. Similarly, the superclasses 'Organoheterocyclic compounds' (indoles, pyridines, quinolines, and derivatives) and 'Benzenoids' (benzene derivatives, phenols) each comprised 28 metabolites. Finally, the superclasses 'Organic Oxygen Compounds' and 'Nucleosides, nucleotides, and analogues' contained 14 and 9 metabolites, respectively.

These finding show that field grown tall wheatgrass root exudates contain a rich diversity of metabolites spanning various superclasses, some of which are recognized for their roles in mediating stress responses, plant-microbe interactions, nutrient cycling, and defense

146 mechanisms. In addition to primary metabolites, we identified a diverse array of secondary
147 metabolites including benzoic acid derivatives, prenol lipids, indoles and derivatives, cinnamic
148 acids, coumarins and flavonoids. Metabolites belonging to these subclasses have been shown to
149 have a role in plant defense, stress response, microbial recruitment, and signaling pathways
150 (Schenkel *et al.*, 2015, Van Poecke *et al.*, 2001, Massalha *et al.*, 2017, Tian et al., 2021, Zhang *et*
151 *al.*, 2009, Hassan & Mathesius, 2012). Among the 224 metabolites that we identified through
152 spectral library matching, we found that 43 have been previously reported (McLaughlin et al.,
153 2023, Zhalnina et al., 2018, Strehmel *et al.*, 2014) in root exudate characterizations of other
154 plants. Notably, 30 of these previously reported metabolites were recently characterized as part
155 of the core exudate metabolome (McLaughlin et al., 2023) in three model plants—*Arabidopsis*

thaliana, Brachypodium distachyon, and *Medicago truncatula*—constituting 40% of the 75-molecule core exudate metabolome. The core metabolites prominently featured nucleobases (adenine, guanine, thymine, uracil) and organic acids, particularly amino acids (asparagine, glutamic acid, glutamine, histidine, leucine, proline, tyrosine), indicating a commonality of these small molecules in exudates across diverse plant species.

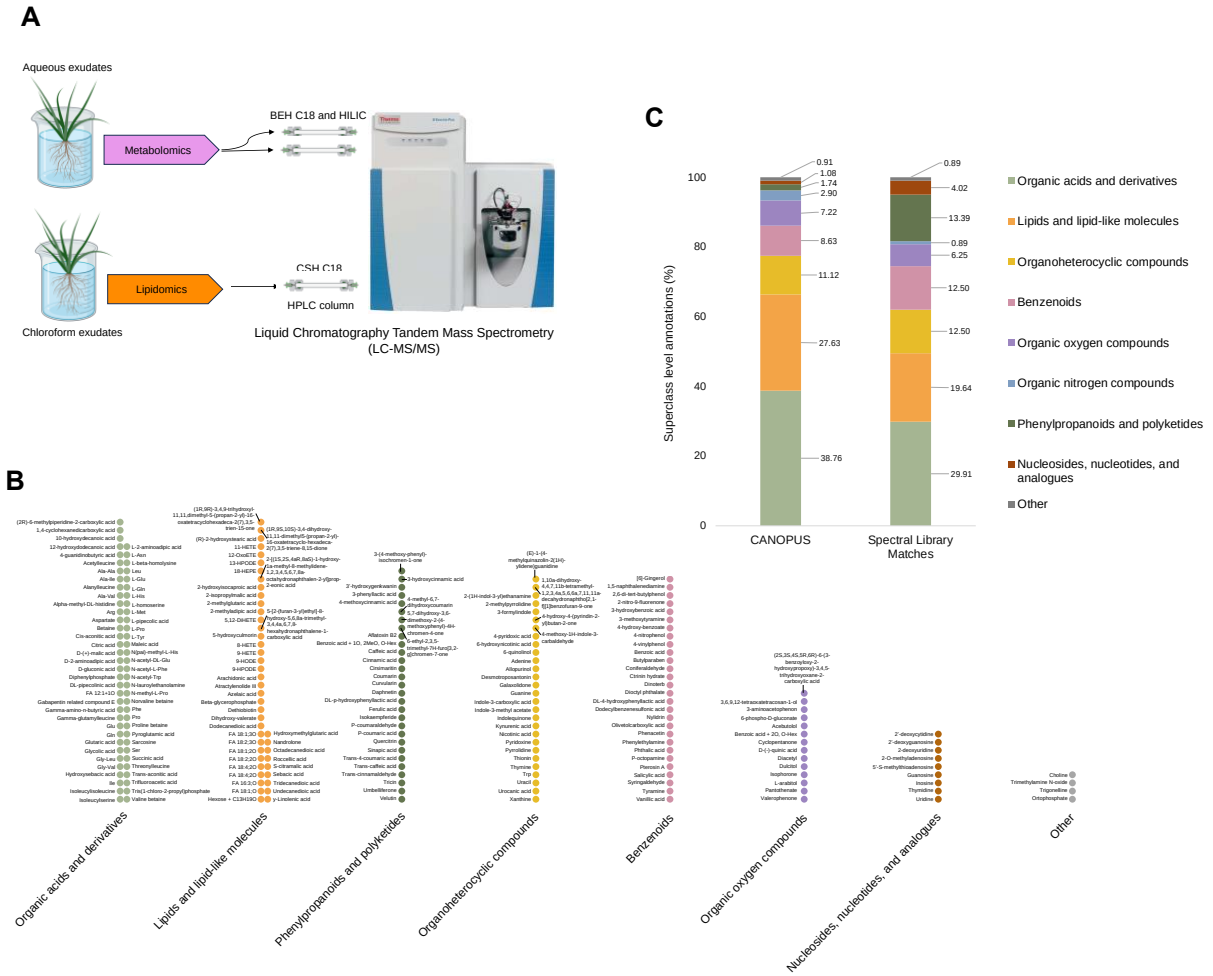

Figure 2: A) Untargeted LC-MS/MS based metabo-lipidomics workflow; B) Metabolites annotated using spectral library searching, colored and listed by superclass C) Percent distribution of superclass level classification of metabolomics features annotated using CANOPUS and spectral library searching (SLS)

While database-dependent methods such as SLS, offer valuable insights into chemical structures, their identification rate is constrained by the library's scope, leaving a substantial majority- often ~90%- of features unannotated (da Silva et al., 2015, Shen et al., 2023). This is a central challenge in the field of metabolomics that needs to be addressed in order to obtain ecological insights from molecular level data (Peters *et al.*, 2018). To maximize the biological information obtained from the unannotated features which are typically discarded from downstream analyses, we complemented SLS with CANOPUS (Dührkop *et al.*, 2021), a deep learning-based class assignment and ontology prediction tool. This enabled the prediction of chemical classifications for 1559 detected, high quality features. It's important to note that due to the higher masses of many lipids, CANOPUS analysis was exclusively applied to the metabolomics data. CANOPUS predicted classifications for 80% of these features spanning 12 superclasses (1205 features classified), 56 classes (1084 features), 85 subclasses (822 features), and 60 level 5 classifications (588 features). Approximately 1250 features received at least one level of classification, substantially increasing our characterization of the chemodiversity of plant exudates. The SLS and CANOPUS analyses uses two separate software (MS-DIAL and MZmine) for feature detection and alignment; it wasn't possible to match features across the analyses. Nonetheless, the combined approach resulted in expanding current knowledge of root exudate chemodiversity.

The superclass-level distribution of annotations from spectral library search (SLS; 224 features) and CANOPUS (1205 features) exhibited similar trends (**Fig 2C**). 'Organic acids and derivatives' predominated in both approaches (SLS 30%, CANOPUS 39%), comprising mainly amino acids, derivatives, and peptides. Following closely was the 'Lipid and lipid-like molecules' superclass (SLS 20%, CANOPUS 28%), where fatty acids and conjugates were prominent. 'Organoheterocyclic compounds' (SLS 12.5%, CANOPUS 11%), 'Benzenoids' (SLS 12.5%, CANOPUS 9%), 'Organic oxygen compounds' (SLS 6%, CANOPUS 7%), including carbohydrates and carbonyl compounds, 'Organic nitrogen compounds' (SLS 1%, CANOPUS 3%), 'Phenylpropanoids and polyketides' (SLS 13%, CANOPUS 2%), and 'Nucleosides, nucleotides, and analogues' (SLS 4%, CANOPUS 1%) followed.

191 **Discovering the Diversity of Lipids in Root Exudates**

192 In the untargeted lipidomics data, 7864 features with MS/MS spectra were detected in positive
193 and negative ionization modes combined. Of these, a mere 289 (~4%) lipid features (including
194 isomers) comprising 267 unique InChIKeys(Heller *et al.*, 2015) were annotated using MS/MS
195 database matching (Schymanski identification confidence level 2A (Schymanski et al., 2014)) with
196 MS-DIAL. Lipids from the glycerolipid and fatty acyl categories were particularly prevalent,
197 followed by sphingolipids, sterol lipids, and glycerophospholipids [**Fig. 3A**]. Known functions of
198 these lipids include diverse roles in membrane structure and stability, energy storage, cell
199 signaling, and responses to stress.

200 In hydrophobic root exudates of mature tall wheatgrass, we found that glycerolipids, particularly
201 triacylglycerols (TG), represent a dominant fraction, comprising 47% of the lipidome. Subclass
202 analysis reveals the prevalence of triradylglycerols (TG), diradylglycerols (DG), and
203 monoradylglycerols (MG) at 33%, 12%, and 2% of annotated lipids, respectively. We examined
204 the distribution of fatty acids within the glycerolipids to identify the top three predominant fatty
205 acids—16:1, 16:0, and 18:1—followed by 18:2, 20:4, 20:5, 20:3, and 24:1, shaping the
206 composition of TG, DG, and MG in root exudates (**Fig 3B**). To approximately quantify glycerolipids
207 in exudates, we spiked a deuterated standard for each subclass. During a 5-minute hydrophobic
208 exudate collection, roots exuded 2 µg of MG, 17.2 µg of DG, and 95.1 µg of TG per gram of fresh
209 root mass. Extrapolating this rate suggests a noteworthy daily exudation of approximately 806 mg
210 of TGs per plant. This calculation represents one of the first approximations of compound-specific
211 exudation rates for mature perennial plants- a central, but missing value that is necessary for
212 quantifying exudate effects on SOM dynamics (citation).

213 Few studies have explored TG lipid secretion in higher plants. A recent study (Tatsumi *et al.*, 2023)
214 revealed significant TG secretion from both cultured cells and hairy roots of *Lithospermum*
215 *erythrorhizon*, with cultured cells secreting about 30% of total TG produced. The authors also
216 observed TG secretion in *N. tabacum* cultured cells and intact plant roots, indicating its
217 occurrence across plant species, consistent with our tall wheatgrass findings. Interestingly, TGs
218 were found to act as carrier lipids, forming lipid droplets that transport other hydrophobic
219 metabolites extracellularly. This confirms that the chemodiversity of root exudate lipids found in

this study is not merely an experimental artifact. While the molecular mechanisms behind TG secretion remain unknown, bayberry (*Myrica pensylvanica*) fruits accumulate TG-rich surface wax through repurposed cutin synthesis genes (Simpson *et al.*, 2016). Diurnal variations in exudation rates (McLaughlin et al., 2023) and the stress induced by the collection protocol may impact TG metabolism and exudation rates, given TGs' role in oxidative stress protection (Fan *et al.*, 2017).

A

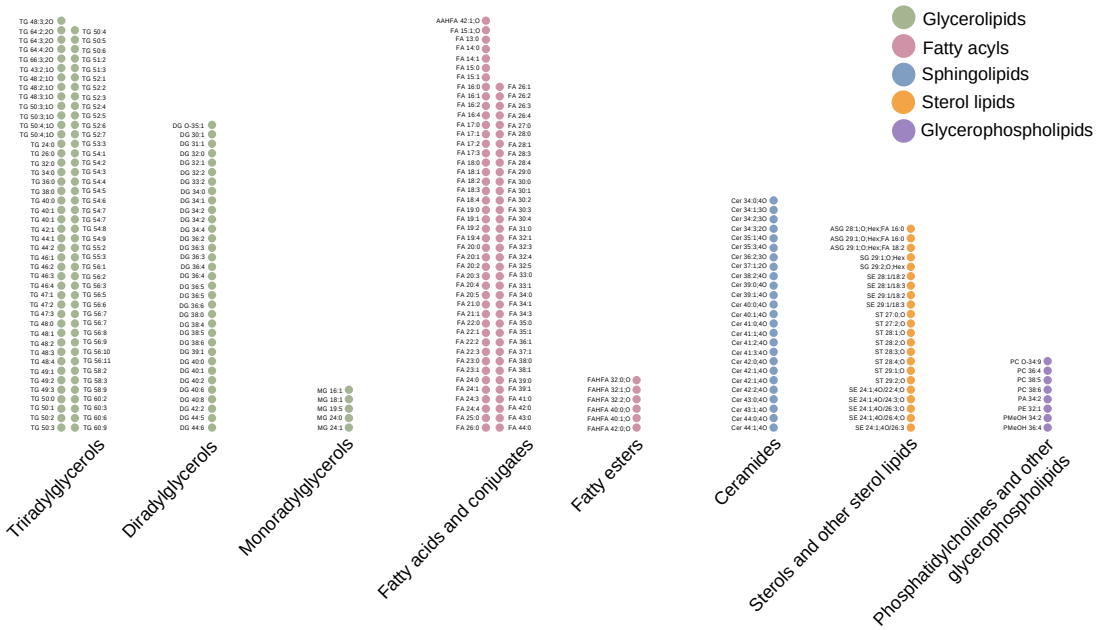

B

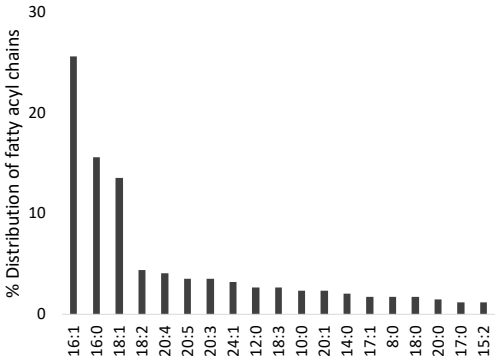

Figure 3: A) Level 2A feature annotations in untargeted lipidomics data; grouped and colored by lipid main class B) Distribution of fatty acid residues in glycerolipids

225 Further investigation into these influences is warranted. In addition to acting as carriers lipids
226 (Tatsumi et al., 2023) we propose that these lipids may influence microbial dynamics, serving as
227 a nutrient source, fostering symbiotic relationships, and impacting the formation and stabilization
228 of water-stable aggregates. Microbial breakdown of lipids such as triacylglycerols in soil would
229 require extracellular enzymes such as esterases and lipases and studies suggest that these lipids
230 may persist longer than simple sugars in soil (Soliman & Radwan, 1981, Hita *et al.*, 1996).
231
232 Amongst the fatty acyl category, 30% of the identified lipids belonged to the subclass of free fatty
233 acids (FA). Fatty acids and derivatives are known to carry out important functions such as
234 stimulating P-solubilizing activity (Pantigoso *et al.*, 2023) and denitrification activity (Lu *et al.*,
235 2014) in rhizosphere bacteria as well as sustaining AMF germination and sporulation (Kameoka &
236 Gutjahr, 2022). However, given the sparse tandem mass spectral fragmentation of FAs, future
237 work needs to confirm the identity of FAs using standards for retention time confirmation and/or
238 gas chromatography coupled with mass spectrometry. Aside from FAs, the remaining fatty acyls
239 consisted of six fatty acyl esters of hydroxy fatty acids (FAHFAs) and one acyl alpha-hydroxy fatty
240 acid (AAHFA). FAHFAs are a recently discovered class of bioactive lipids found in plants, yeast, and
241 mammals, some of which exhibit anti-inflammatory and anti-diabetic activity (Kolar *et al.*, 2019,
242 Yore *et al.*, 2014). The role of these lipids in root exudates is still unknown.
243
244 Sphingolipids—specifically ceramides—made up 9% of the annotated lipids [**Fig. 2A**]. Ceramides
245 serve many functions in plants, including cell signaling, stress response, and membrane integrity.
246 The biophysical properties and functions of ceramides can vary depending on the constituent
247 sphingoid base and fatty acid. The ceramides we detected were largely composed of trihydroxy
248 long chain bases (LCB) 18:0 and 18:1 (48% and 16% of the ceramides respectively) and α-hydroxy
249 fatty acids varying in length from 16 to 26 carbons which are typical in plants (Lynch & Dunn,
250 2004). Isolated LCBs have been shown to inhibit the growth of plant-associated fungi and bacteria
251 *(Glenz et al., 2022).* Ceramides in other host-microbe ecosystems such as human skin are known
252 to inhibit pathogenic biofilm formation (Cleary *et al.*, 2018). The functions of ceramides in root
253 exudates are yet to be elucidated, but their potential roles in regulating the growth of plant-

254 associated microbes and biofilms warrant further investigation given their abundance in root
255 exudates.
256
257 Phytosterols, accounting for 8% of identified lipids, play key roles in plant-microbe interactions
258 and plant health. We identified stigmasterol, a plant sterol with demonstrated potential for
259 improving nitrogen use efficiency in the rhizosphere. A recent study revealed that a denitrifying
260 bacterial inoculant strain could influence stigmasterol concentrations in duckweed root exudates
261 leading to increased nitrite reductase activity, biofilm formation, and promotion of plant growth
262 (Lu *et al.*, 2021). Only eight glycerophospholipids (3%) were identified and these included
263 phosphatidylcholines and phosphatidylethanolamine which are abundant phospholipids in plant
264 cell membranes. The low number of phospholipids detected suggests that the hydrophobic
265 exudate collection protocol used in this study effectively captured lipids arising from root
266 exudates rather than from root cell membranes or surface attached microbial cells.
267
268 **Comparison of the Root Exudate Lipidome with the Root Tissue Lipidome**
269 We used untargeted LC-MS/MS lipidomics to characterize lipids in root tissue and compared root
270 tissue and exudate lipid composition. In root tissue, 539 lipid features (including isomers)
271 comprising 503 unique InChIKeys were annotated using MS/MS database matching (Schymanski
272 identification confidence level 2A) with MS-DIAL. Lipids from the glycerolipid,
273 glycerophospholipid, fatty acyl, sphingolipid, and sterol lipid categories were detected [**Fig. 4A**].
274 Upon comparing lipids detected in root exudates and root tissue, we found that amongst a total
275 of 594 lipids, 327 were only detected in roots, 91 were only detected in root exudates and 176
276 were detected in both roots and root exudates [**Fig. 4B**]. Although it is unclear why certain
277 molecules were detected in exudates but not in root tissue, this has been observed previously by
278 others (McLaughlin et al., 2023). A breakdown of lipids by category, unique to roots or exudates
279 or those detected in both is shown in **Fig. 4C.** While only 8 glycerophospholipids were detected
280 in exudates, 102 glycerophospholipids were detected in root tissue. We examined the distribution
281 of fatty acyl chains in the triacylglycerols and found that in TGs detected only in the roots, 18:2

282 was predominant (51% of all fatty acyl chains) followed by 18:1 (22%) and 18:3 (22%).
283 Interestingly, in TGs detected only in the exudates, 20:3 constituted 9% of the fatty acyl chains,

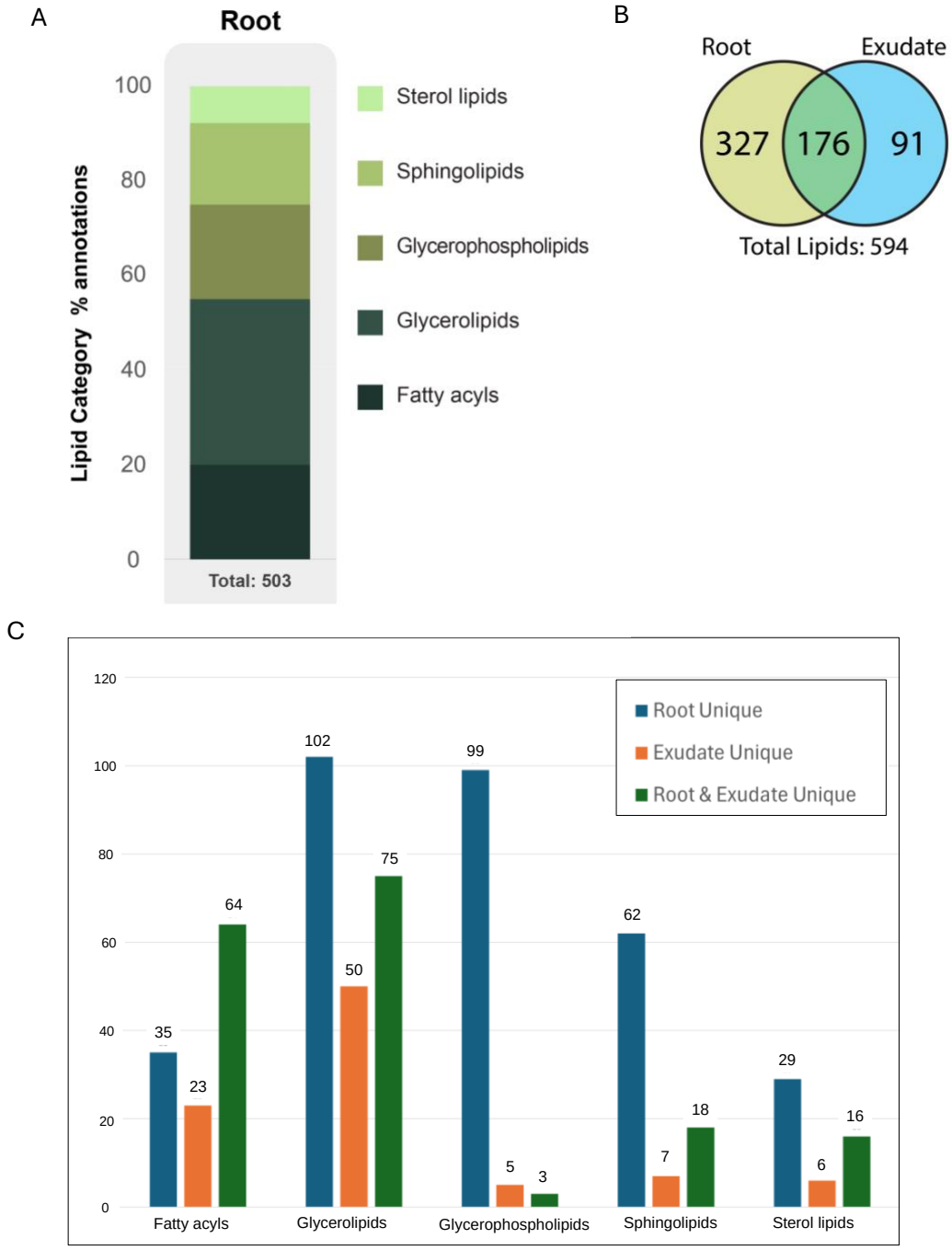

Figure 4: A) Percent distribution of lipid categories of lipids identified in roots B) Venn diagram of unique and overlapping lipids identified in root tissue and exudates C) Breakdown of number of unique and overlapping lipids identified in roots and exudates by lipid category

284 while it was not present in any of the TGs detected in only the roots. Detailed lists of all identified
285 lipids and metabolites in this study can be found in the **Supplementary Files**.
286
287 **Conclusions and Future Directions**
288 A comprehensive characterization of small molecules-including lipids-in root exudates is a critical
289 first step for advancing our understanding of the functions and fate of rhizodeposits in terrestrial
290 ecosystems. Using mature, field-grown tall wheatgrass plants as a case study, we demonstrate
291 the first comprehensive characterization of the root exudate metabo-lipidome. We found that C
292 input rates in hydrophobic exudates were around double that of aqueous exudates and C/N ratios
293 were markedly higher in hydrophobic exudates when compared to aqueous (459 ± 90 vs 14.40 ±
294 0.58). Despite the caveat that there may be variations in exudation in undisturbed soil
295 environments and our collection methods that use water and chloroform, these findings
296 emphasize the need to pay closer attention to the lipid fraction of root exudates and highlight the
297 need to investigate the impact of exudate lipids on microbial physiology, carbon use efficiency,
298 and SOM formation and turnover. In an unprecedented characterization of intact lipids in root
299 exudates, our results reveal the presence of a variety of lipids with diverse functions, with
300 substantial levels of triacylglycerols which previously were not known to be exuded by roots. The
301 combined use of SLS and CANOPUS strategies for metabolite identification, not only enabled high
302 confidence annotations via spectral library searches but also facilitated a broader assignment of
303 chemical class information across detected features. This dual strategy, leveraging the strengths
304 of both methods, enhanced the depth and coverage of metabolite identification, contributing to
305 a more thorough understanding of the exudate metabolome. Overall, with 513 metabolite and
306 lipid identifications and chemical classification of 1250 features (~80% of all high-quality features
307 detected), this work represents the most comprehensive molecular characterization of root
308 exudates so far.
309
310 Achieving sustainable and climate-resilient ecosystems requires an understanding of the impact
311 of root exudates on microbial community functions and soil carbon dynamics. The findings in this
312 work will be critical in resolving current uncertainties in quantifying plant contributions to SOM

formation and stabilization. Future studies need to quantify the impacts of environmental factors (climate, soil properties) on the exudate metabo-lipidome, and evaluate the functional consequences of various small molecules on microbial metabolism and activity. Leveraging the findings in this work, targeted incubations with exudate metabolites and lipids can be designed to understand the effect of these molecules on microbial metabolism and their interactions with minerals. The impact and contributions of root endophytes and symbionts such as arbuscular mycorrhizal fungi on exudate chemistry is not known and warrants interrogation. Investigations on priming can incorporate increasingly complex mixtures or natural exudates to understand microbial community responses in realistic conditions. Comprehensive molecular mapping of the soil metabo-lipidome, by systematic characterization of small molecule metabolites and lipids from plant and microbial sources, and their cross-feeding between organisms, is essential for understanding interactions and metabolic pathways that drive ecological functions such as SOM formation and nutrient cycling.

As we navigate the open frontier of exploring the functions of lipids in root exudates and soil ecosystems, particularly their potential to enhance plant health, long-term storage of soil carbon and ecosystem resilience, the identification of key bioactive exudate metabolites and lipids becomes paramount. This knowledge can inform breeding of desired plant traits to facilitate plant-microbe partnerships that can enhance plant productivity and stress tolerance, all while promoting soil carbon storage. In essence, understanding the complex interplay between lipids in root exudates and soil microbial communities provides valuable insights for sustainable agricultural practices and biofeedstock ecosystem management.

Methods

Plant harvest and exudate collection:

Five mature tall wheatgrass (*Thinopyrum ponticum*, cultivar: Alkar) plant bunches were harvested in October 2022 from our Tall Wheatgrass Field Trial site at Washington State University (WSU)-Irrigated Agriculture Research and Extension Center (WSU-IAREC) in Prosser, WA, USA. These plants were established in 2018 and were allowed to grow for ~4 years under normal irrigation conditions. Plants were harvested along with their intact roots and the surrounding soil using a shovel to unearth a root ball that was approximately 30 cm wide x 30 cm deep. After gentle removal of root-associated soil, plant roots were washed in MilliQ water by submerging and shaking gently to remove any remaining soil. After washing, the plants were transferred to 5 L glass beakers where their roots were submerged in 1.5 L of pure milliQ water for 2 hours. The aqueous exudate solutions were vacuum filtered at 0.22 µm and aliquoted into 50 mL tubes for storage at -80 C. Subsequently, the plants roots were transferred to 5 L glass beakers where their roots were submerged in 500 mL chloroform for 5 minutes to collect hydrophobic lipids in exudates. The chloroform exudates were aliquoted into 50 mL tubes for storage at -80 C. 25 mL of aqueous or chloroform exudates were vacuum dried and reconstituted for downstream metabolomics and lipidomics analysis respectively.

Root samples were lyophilized prior to lipid extractions using a modified Folch extraction known as MPLEx (Nakayasu *et al.*, 2016, Nicora *et al.*, 2018). Lyophilized root samples were ground into a fine powder using a GenoGrinder and 200 mg of powdered sample was used for extraction. Briefly, 5 mL of cold 2:1 (v/v) mixture of chloroform: methanol was added to each sample followed by vortexing. Then 1 mL of cold Milli-Q water was added and samples were vortexed for 1 min. Samples were allowed to cool on ice followed by addition of 1 mL of cold Milli-Q water and vortexing for 1 min. Samples were centrifuged at 4,000 g for 5 min at 4°C resulting in separation into three defined upper layers, the upper-most aqueous (metabolite) layer, the protein interlayer and the lower organic (lipid) layer with the remaining debris at the bottom. The polar metabolite and lipid fractions were collected separately and dried down.

366

367 **Mass spectrometry (LC-MS/MS) analysis**:

368 Metabolites were analyzed using reverse phase (RP) and hydrophilic interaction chromatography
369 (HILIC) separations on a Thermo Fisher Scientific HF-X mass spectrometer (Thermo Scientific, San
370 Jose, CA) coupled with a Waters Acquity UPLC H class liquid chromatography system (Waters
371 Corp., Milford, MA). Metabolites were brought up in 200 uL of 50% LCMS grade methanol and
372 50% nanopure water. RP separation was performed by injecting 5 uL of sample onto a Thermo
373 Scientific Hypersil GOLD C18 column (3 µm, 2.1 mm ID X 150 mm L) heated to 40°C. Metabolites
374 were separated using an 18 minute gradient with data collected on the first 17 minutes. The RP
375 mobile phase A consisted of 0.1% formic acid in nanopure water and a mobile phase B consisting
376 of 0.1% formic acid in LCMS grade acetonitrile. The gradient used was as follows (min, flowrate in
377 mL/min, %B): 0,0.4,10; 2,0.4,10; 11,0.4,90; 12,0.4,90; 12.5,0.5,90; 13.5,0.5,10; 14,0.5,10;
378 14.5,0.4,10; 15,0.4,10. Positive and negative ion modes were analyzed in separate injections.
379 HILIC separation was performed by injecting 3 uL of sample onto a Waters Acquity BEH Amide
380 column (130 Å, 1.7 µm, 2.1 mm ID X 100 mm L) heated to 55°C. Metabolites were separated
381 using a 16 minute gradient with data collected for the first 15 minutes. The HILIC mobile phase A
382 consisted of 0.05% ammonium hydroxide, 5% LCMS grade acetonitrile, and 94.95% 10 mM
383 ammonium acetate in nanopure water with a mobile phase B consisting of 0.05% ammonium
384 hydroxide in 99.95% LCMS grade acetonitrile. The gradient used was as follows (min, flowrate in
385 mL/min, %B): 0,0.3,95; 6,0.3,37; 7,0.3,37; 7.1,0.3,95; 7.2,0.5,95; 9.5,0.5,95; 9.7,0.3,95; 16,0.3,95.
386 Positive and negative ion modes were analyzed in separate injections. For both RP and HILIC
387 separations the Thermo Fisher Scientific HF-X was equipped with a HESI source and high flow
388 needle with the following parameters: spray voltage of 3.6 kV in positive mode and 3kV in
389 negative mode, capillary temperature of 300°C, probe heater temp of 370°C, sheath gas at 60
390 L/min, auxiliary gas at 25 L/min, and spare gas at 2 L/min. Metabolites were analyzed at a
391 resolution of 60 k and a scan range of 50 to 750 m/z for parent ions followed by MS/MS HCD
392 fragmentation which is data dependent on the top 4 ions with a resolution of 15 K and stepped
393 normalized collision energies of 20, 30, and 40. Total organic carbon (TOC) and total nitrogen (TN)

394 in metabolite extracts were measured in acidified extracts on a Vario TOC cube (Elementar,
395 Germany). C/N ratio was calculated by the ratio of TOC and TN.

396 Lipid extracts were analyzed by RP separation using a Waters Aquity UPLC H class system
397 (Waters Corp., Milford, MA) coupled with a LTQ Velos Elite Orbitrap mass spectrometer (Thermo
398 Scientific, San Jose, CA). Samples were stored in 2 parts chloroform and 1 part methanol, were
399 evaporated, and reconstituted in 100 µL of 90% methanol and 10% chloroform prior to injecting
400 10 µl onto a Waters column (CSH 3.0 mm x 150 mm x 1.7 µm particle size) heated to 42°C. Lipids
401 were then separated using a 42 min gradient with data collected on the first 34 minutes. Mobile
402 phase A consisted of 10mM ammonium acetate in 60% nanopure water and 40% LCMS grade
403 acetonitrile with a mobile phase B consisting of 10 mM ammonium acetate in 90% LCMS grade
404 isopropanol and 10% LCMS grade acetonitrile. The gradient used for both positive and negative
405 mode was as follows (min, flowrate, %B): 0,0.25,40; 2,0.25,50; 3,0.25,60; 12,0.25,70; 15,0.25,75;
406 17,0.25,78, 19,0.25,85; 22,0.25,92; 25,0.25,99; 34,0.25,99; 34.5,0.3,99; 35,0.3,99; 35.5,0.3,99;
407 36,0.35,40; 37,0.3,40; 38,0.25,40. A Thermo HESI source was coupled to the mass spectrometer
408 inlet with both heated to 350°C with a spray voltage of 3.5 kV and sheath, auxiliary, and sweep
409 gas flows of 45, 30, and 2, respectively. Positive and negative polarities were analyzed in separate
410 sample runs. Lipids were fragmented by both HCD and CID using a parent ion scan of 200-2000
411 m/z with a 60 k resolving power. Subsequent MS/MS was performed on the top 4 ions. An
412 isolation width of 2 m/z units and a maximum charge state of 2 were used for both CID and HCD
413 scans. A normalized collision energy of 35 was used for CID while 30 was used for HCD. CID spectra
414 were acquired in the ion trap using an activation Q value of 0.18, while HCD spectra were acquired
415 in the Orbitrap at a mass resolution of 7.5 k and a first fixed mass of m/z 90. For quantification of
416 glycerolipids, a sample was spiked with EquiSPLASH lipid mix (Avanti Polar Lipids) containing
417 deuterated TG, DG and MG internal standards and run in positive and negative mode with each
418 injection containing 0.1 µg of each standard. The area under the peak for the standards was used
419 for quantifying the total amount of lipids of the same lipid class in the samples. Total carbon (TC)
420 and nitrogen (TN) content in lipid extracts was quantified after drying down extracts in tin
421 capsules by using an Elementar Vario Isotope cube elemental analyzer (Elementar, Germany). C/N

422 ratio was calculated by the ratio of TC and TN. Chloroform blanks were analyzed alongside
423 samples to control for residual C contributed by the solvent.
424
425 Data processing: Metabolite and lipid identifications were made using MS-DIAL v4.92 for peak
426 detection, identification and alignment. For metabolomics, the experimental data was matched
427 both to in-house libraries (m/z less than 0.003 Da, retention time less than 0.3 min, MS/MS
428 spectral match) and a compilation of publicly available MS/MS databases (m/z less than 0.003 Da,
429 MS/MS spectral match) (VS17) available in the MS-DIAL metabolomics MSP spectral kit
430 (http://prime.psc.riken.jp/compms/msdial/main.html#MSP). The tandem mass spectra and
431 corresponding fragment ions, mass measurement error, and aligned chromatographic features
432 were manually examined to remove false positives. Relative quantification was performed by
433 calculating peak areas on extracted ion chromatograms of precursor masses. Features detected
434 in at least three of the five replicates were retained.
435
436 Although confident structural identification of features remains a central goal of metabolomics
437 and lipidomics, it is useful to note that a considerable fraction of features detected in untargeted
438 mass-spectrometry based analyses can arise due to artifacts such as in-source fragments,
439 adducts, isotopes, and contaminants and may not all be biological, unique or informative (Peisl
440 *et al.*, 2018). To prepare metabolomics data for CANOPUS analysis, Proteowizard (Chambers *et*
441 *al.*, 2012) and MZmine3 (Schmid *et al.*, 2023) were used on each mode separately. Raw data was
442 centroided, peak-picked, and converted to compatible formats with Proteowizard. Resulting
443 mzML files were imported into MZmine3 and underwent noise cancellation and automated data
444 analysis pipeline (ADAP) chromatogram generation. Noise intensity levels were set at 6.0E3–8.0E3
445 a.u. (arbitrary units) for MS2 spectra and 6.0E4–1.0E5 a.u. for MS1. The local minimum resolver
446 was manually adjusted to reduce peak broadening and splitting; only significant peaks in the
447 chromatograms were recognized as features. Minimum absolute peak height was set to 1.5E5–
448 2.5E5 a.u. across the modes. 13C related peaks within the same feature list were removed such
449 that only the most significant isotope remained. The isotope pattern finder was also used to
450 detect stable isotopes of hydrogen, carbon, nitrogen, oxygen, sulfur, and phosphorus. Deisotoped

feature lists were aligned to produce one feature list with data from the entire mode. Further analysis filtered out rows with less than two features present and remaining ^{13}C isotopes. Finally, as feature detection steps (e.g. peak height below minimum intensity, alignment errors, etc.) may result in lost peaks, gap filling was performed. The resulting aligned, filtered, and gap-filled feature list of each mode was exported as an MGF file. Molecular networking files were saved for downstream analysis. A total of 1559 high quality features with MS2 scans were obtained across the 4 modes.

MGF files were transferred to SIRIUS 5.7.2. (Duhrkop *et al.*, 2019) for CANOPUS analysis. CANOPUS utilized the fragmentation trees and molecular fingerprints to predict ClassyFire classifications of features (Djoumbou Feunang *et al.*, 2016, Duhrkop *et al.*, 2021). Classifications with certainties/confidence below 75% were discarded. Summaries were exported with CANOPUS ClassyFire predictions.

Funding and Acknowledgements

PNNL is a multi-program national laboratory operated by Battelle for the DOE under Contract DE-AC05-76RLO 1830. This program is supported by the U. S. Department of Energy, Office of Science, through the Genomic Science Program, Office of Biological and Environmental Research, under FWP 70880. A portion of this work was performed in the William R. Wiley Environmental Molecular Sciences Laboratory (EMSL), a national scientific user facility sponsored by the Office of Biological and Environmental Research and located at PNNL. IY and DH were supported by the DOE Office of Science's Science Undergraduate Laboratory Internship (SULI) program. The authors thank Jayde Aufrecht, Daisy Herrera, Sharon Zhao, Eric Garza, Meagan Burnet and Jesse Trejo for assisting with root exudate sample collection following the plant harvest, Sophia McKever and Kaizad Patel for assistance with TC/TN measurements and Shannon Sheridan for helping curate the data package on DataHub.

Author Contributions

SPC conceived the initial idea and SPC and KSH designed the study. SPC and SLB carried out field collection of plants and exudates. SLB measured TC and TN content in samples. JE collected the

LC-MS/MS data on the instrument and helped with glycerolipid quantification. SPC and IY analyzed the metabolomics and lipidomics data and wrote the initial draft of the manuscript. DH analyzed the root tissue lipidomics data. All authors contributed to produce the final draft. KSH obtained the funding.

Data Availability

Primary raw mass spectrometry lipidomics and metabolomics data have been deposited at MassIVE under the accession: MSV000093600 (will be made public after peer-review when manuscript is accepted for publication).

Competing interest statement: The authors declare that they have no known conflicts of interest or competing financial interests that influence this work.

References

BADRI, D. V. and VIVANCO, J. M. (2009) Regulation and function of root exudates. *Plant, Cell & Environment,* **32,** 666-681.

Brown, R. W., Reay, M. K., Centler, F., Chadwick, D. R., Bull, I. D., McDonald, J. E.*, et al.* (2024) Soil metabolomics - current challenges and future perspectives. *Soil Biology and Biochemistry,* **193,** 109382.

Chagas, F. O., Pessotti, R. d. C., Caraballo-Rodríguez, A. M. and Pupo, M. T. (2018) Chemical signaling involved in plant–microbe interactions. *Chemical Society Reviews,* **47,** 1652-1704.

Chambers, M. C., Maclean, B., Burke, R., Amodei, D., Ruderman, D. L., Neumann, S.*, et al.* (2012) A cross-platform toolkit for mass spectrometry and proteomics. *Nat Biotechnol,* **30,** 918-920.

Chen, L., Liu, L., Qin, S., Yang, G., Fang, K., Zhu, B.*, et al.* (2019) Regulation of priming effect by soil organic matter stability over a broad geographic scale. *Nature Communications,* **10,** 5112.

Cleary, J. M., Lipsky, Z. W., Kim, M., Marques, C. N. H. and German, G. K. (2018) Heterogeneous ceramide distributions alter spatially resolved growth of Staphylococcus aureus on human stratum corneum. *J R Soc Interface,* **15**.

Couvillion, S. P., Danczak, R. E., Naylor, D., Smith, M. L., Stratton, K. G., Paurus, V. L.*, et al.* (2023) Rapid remodeling of the soil lipidome in response to a drying-rewetting event. *Microbiome,* **11,** 34.

da Silva, R. R., Dorrestein, P. C. and Quinn, R. A. (2015) Illuminating the dark matter in metabolomics. *Proceedings of the National Academy of Sciences,* **112,** 12549-12550.

de Vries, F. T., Williams, A., Stringer, F., Willcocks, R., McEwing, R., Langridge, H.*, et al.* (2019) Changes in root-exudate-induced respiration reveal a novel mechanism through which drought affects ecosystem carbon cycling. *New Phytol,* **224,** 132-145.

Dietz, S., Herz, K., Döll, S., Haider, S., Jandt, U., Bruelheide, H.*, et al.* (2019) Semi-polar root exudates in natural grassland communities. *Ecology and Evolution,* **9,** 5526-5541.

Djoumbou Feunang, Y., Eisner, R., Knox, C., Chepelev, L., Hastings, J., Owen, G.*, et al.* (2016) ClassyFire: automated chemical classification with a comprehensive, computable taxonomy. *J Cheminform,* **8,** 61.

Duhrkop, K., Fleischauer, M., Ludwig, M., Aksenov, A. A., Melnik, A. V., Meusel, M.*, et al.* (2019) SIRIUS 4: a rapid tool for turning tandem mass spectra into metabolite structure information. *Nat Methods,* **16,** 299-302.

Dührkop, K., Nothias, L.-F., Fleischauer, M., Reher, R., Ludwig, M., Hoffmann, M. A.*, et al.* (2021) Systematic classification of unknown metabolites using high-resolution fragmentation mass spectra. *Nature Biotechnology,* **39,** 462-471.

Duhrkop, K., Nothias, L. F., Fleischauer, M., Reher, R., Ludwig, M., Hoffmann, M. A.*, et al.* (2021) Systematic classification of unknown metabolites using high-resolution fragmentation mass spectra. *Nat Biotechnol,* **39,** 462-471.

Elias, K. S. and Safir, G. R. (1987) Hyphal Elongation of Glomus fasciculatus in Response to Root Exudates. *Applied and Environmental Microbiology,* **53,** 1928-1933.

Fan, J., Yu, L. and Xu, C. (2017) A Central Role for Triacylglycerol in Membrane Lipid Breakdown, Fatty Acid β-Oxidation, and Plant Survival under Extended Darkness. *Plant Physiol,* **174,** 1517-1530.

Fontaine, S., Barot, S., Barré, P., Bdioui, N., Mary, B. and Rumpel, C. (2007) Stability of organic carbon in deep soil layers controlled by fresh carbon supply. *Nature,* **450,** 277-280.

Giera, M., Yanes, O. and Siuzdak, G. (2022) Metabolite discovery: Biochemistry's scientific driver. *Cell Metab.,* **34,** 21-34.

Glenz, R., Kaiping, A., Gopfert, D., Weber, H., Lambour, B., Sylvester, M.*, et al.* (2022) The major plant sphingolipid long chain base phytosphingosine inhibits growth of bacterial and fungal plant pathogens. *Sci Rep,* **12,** 1081.

Hassan, S. and Mathesius, U. (2012) The role of flavonoids in root-rhizosphere signalling: opportunities and challenges for improving plant-microbe interactions. *J Exp Bot,* **63,** 3429-3444.

Heller, S. R., McNaught, A., Pletnev, I., Stein, S. and Tchekhovskoi, D. (2015) InChI, the IUPAC International Chemical Identifier. *J Cheminform,* **7,** 23.

Heuermann, D., Döll, S., Schweneker, D., Feuerstein, U., Gentsch, N. and von Wirén, N. (2023) Distinct metabolite classes in root exudates are indicative for field- or hydroponically-grown cover crops. *Front Plant Sci,* **14,** 1122285.

Hita, C., Parlanti, E., Jambu, P., Joffre, J. and Amblès, A. (1996) Triglyceride degradation in soil. *Organic Geochemistry,* **25,** 19-28.

Huang, A. C., Jiang, T., Liu, Y.-X., Bai, Y.-C., Reed, J., Qu, B.*, et al.* (2019) A specialized metabolic network selectively modulates Arabidopsis root microbiota. *Science,* **364,** eaau6389.

Hugoni, M., Luis, P., Guyonnet, J. and Haichar, F. e. Z. (2018) Plant host habitat and root exudates shape fungal diversity. *Mycorrhiza,* **28,** 451-463.

Jansson, J. K. and Hofmockel, K. S. (2018) The soil microbiome—from metagenomics to metaphenomics. *Current Opinion in Microbiology,* **43,** 162-168.

Kallenbach, C. M., Frey, S. D. and Grandy, A. S. (2016) Direct evidence for microbial-derived soil organic matter formation and its ecophysiological controls. *Nature Communications,* **7,** 13630.

Kameoka, H. and Gutjahr, C. (2022) Functions of Lipids in Development and Reproduction of Arbuscular Mycorrhizal Fungi. *Plant Cell Physiol,* **63,** 1356-1365.

Khalid, S. and Keller, N. P. (2021) Chemical signals driving bacterial–fungal interactions. *Environmental Microbiology,* **23,** 1334-1347.

Kolar, M. J., Konduri, S., Chang, T., Wang, H., McNerlin, C., Ohlsson, L.*, et al.* (2019) Linoleic acid esters of hydroxy linoleic acids are anti-inflammatory lipids found in plants and mammals. *Journal of Biological Chemistry,* **294,** 10698-10707.

Liang, G., Stark, J. and Waring, B. G. (2023) Mineral reactivity determines root effects on soil organic carbon. *Nature Communications,* **14,** 4962.

Lu, Y., Kronzucker, H. J. and Shi, W. (2021) Stigmasterol root exudation arising from Pseudomonas inoculation of the duckweed rhizosphere enhances nitrogen removal from polluted waters. *Environmental Pollution,* **287,** 117587.

Lu, Y., Zhou, Y., Nakai, S., Hosomi, M., Zhang, H., Kronzucker, H. J.*, et al.* (2014) Stimulation of nitrogen removal in the rhizosphere of aquatic duckweed by root exudate components. *Planta,* **239,** 591-603.

Lynch, D. V. and Dunn, T. M. (2004) An introduction to plant sphingolipids and a review of recent advances in understanding their metabolism and function. *New Phytologist,* **161,** 677-702.

Mark, G. L., Dow, J. M., Kiely, P. D., Higgins, H., Haynes, J., Baysse, C.*, et al.* (2005) Transcriptome profiling of bacterial responses to root exudates identifies genes involved in microbe-plant interactions. *Proceedings of the National Academy of Sciences,* **102,** 17454-17459.

Massalha, H., Korenblum, E., Tholl, D. and Aharoni, A. (2017) Small molecules below-ground: the role of specialized metabolites in the rhizosphere. *Plant J,* **90,** 788-807.

McLaughlin, S., Zhalnina, K., Kosina, S., Northen, T. R. and Sasse, J. (2023) The core metabolome and root exudation dynamics of three phylogenetically distinct plant species. *Nature Communications,* **14,** 1649.

Monge, M. E., Dodds, J. N., Baker, E. S., Edison, A. S. and Fernández, F. M. (2019) Challenges in Identifying the Dark Molecules of Life. *Annu Rev Anal Chem (Palo Alto Calif),* **12,** 177-199.

Naasko, K. I., Naylor, D., Graham, E. B., Couvillion, S. P., Danczak, R., Tolic, N.*, et al.* (2023) Influence of soil depth, irrigation, and plant genotype on the soil microbiome, metaphenome, and carbon chemistry. *mBio,* **14,** e01758-01723.

Nakayasu, E. S., Nicora, C. D., Sims, A. C., Burnum-Johnson, K. E., Kim, Y.-M., Kyle, J. E.*, et al.* (2016) MPLEx: a robust and universal protocol for single-sample integrative proteomic, metabolomic, and lipidomic analyses. *MSystems,* **1,** e00043-00016.

Naveed, M., Brown, L. K., Raffan, A. C., George, T. S., Bengough, A. G., Roose, T.*, et al.* (2017) Plant exudates may stabilize or weaken soil depending on species, origin and time. *European Journal of Soil Science,* **68,** 806-816.

Nicora, C. D., Burnum-Johnson, K. E., Nakayasu, E. S., Casey, C. P., White, R. A., 3rd, Roy Chowdhury, T.*, et al.* (2018) The MPLEx Protocol for Multi-omic Analyses of Soil Samples. *J Vis Exp***,** 57343.

Pantigoso, H. A., Manter, D. K., Fonte, S. J. and Vivanco, J. M. (2023) Root exudate-derived compounds stimulate the phosphorus solubilizing ability of bacteria. *Scientific Reports,* **13,** 4050.

Peisl, B. Y. L., Schymanski, E. L. and Wilmes, P. (2018) Dark matter in host-microbiome metabolomics: Tackling the unknowns–A review. *Analytica Chimica Acta,* **1037,** 13-27.

Peters, K., Worrich, A., Weinhold, A., Alka, O., Balcke, G., Birkemeyer, C.*, et al.* (2018) Current Challenges in Plant Eco-Metabolomics. *Int J Mol Sci,* **19,** 1385.

Phillips, R. P., Erlitz, Y., Bier, R. and Bernhardt, E. S. (2008) New approach for capturing soluble root exudates in forest soils. *Functional Ecology,* **22,** 990-999.

Rempfert, K. R., Bell, S. L., Kasanke, C. P., Zhao, Q., Zhao, X., Lipton, A. S.*, et al.* (2024) Biomolecular budget of persistent, microbial-derived soil organic carbon: The importance of underexplored pools. *Science of The Total Environment,* **932,** 172916.

Sasse, J., Martinoia, E. and Northen, T. (2018) Feed Your Friends: Do Plant Exudates Shape the Root Microbiome? *Trends in Plant Science,* **23,** 25-41.

Schenkel, D., Lemfack, M. C., Piechulla, B. and Splivallo, R. (2015) A meta-analysis approach for assessing the diversity and specificity of belowground root and microbial volatiles. *Front Plant Sci,* **6,** 707.

Schmid, R., Heuckeroth, S., Korf, A., Smirnov, A., Myers, O., Dyrlund, T. S.*, et al.* (2023) Integrative analysis of multimodal mass spectrometry data in MZmine 3. *Nat Biotechnol,* **41,** 447-449.

Schymanski, E. L., Jeon, J., Gulde, R., Fenner, K., Ruff, M., Singer, H. P.*, et al.* (2014) Identifying Small Molecules via High Resolution Mass Spectrometry: Communicating Confidence. *Environmental Science & Technology,* **48,** 2097-2098.

Shen, S., Zhan, C., Yang, C., Fernie, A. R. and Luo, J. (2023) Metabolomics-centered mining of plant metabolic diversity and function: Past decade and future perspectives. *Molecular Plant,* **16,** 43-63.

Simon, L. and Haichar, F. E. Z. (2019) Determination of Root Exudate Concentration in the Rhizosphere Using (13)C Labeling. *Bio Protoc,* **9,** e3228.

Simpson, J. P., Thrower, N. and Ohlrogge, J. B. (2016) How did nature engineer the highest surface lipid accumulation among plants? Exceptional expression of acyl-lipid-associated genes for the assembly of extracellular triacylglycerol by Bayberry (Myrica pensylvanica) fruits. *Biochimica et Biophysica Acta (BBA) - Molecular and Cell Biology of Lipids,* **1861,** 1243-1252.

Soliman, A. H. and Radwan, S. S. (1981) Degradation of Sterols, Triacylglycerol, and Phospholipids by Soil Microorganisms. *Zentralblatt für Bakteriologie, Parasitenkunde, Infektionskrankheiten und Hygiene. Zweite Naturwissenschaftliche Abteilung: Mikrobiologie der Landwirtschaft, der Technologie und des Umweltschutzes,* **136,** 420-426.

Strehmel, N., Böttcher, C., Schmidt, S. and Scheel, D. (2014) Profiling of secondary metabolites in root exudates of Arabidopsis thaliana. *Phytochemistry,* **108,** 35-46.

Tatsumi, K., Ichino, T., Isaka, N., Sugiyama, A., Moriyoshi, E., Okazaki, Y.*, et al.* (2023) Excretion of triacylglycerol as a matrix lipid facilitating apoplastic accumulation of a lipophilic metabolite shikonin. *Journal of Experimental Botany,* **74,** 104-117.

Tian, B., Pei, Y., Huang, W., Ding, J. and Siemann, E. (2021) Increasing flavonoid concentrations in root exudates enhance associations between arbuscular mycorrhizal fungi and an invasive plant. *Isme j,* **15,** 1919-1930.

Van Poecke, R. M., Posthumus, M. A. and Dicke, M. (2001) Herbivore-induced volatile production by Arabidopsis thaliana leads to attraction of the parasitoid Cotesia rubecula: chemical, behavioral, and gene-expression analysis. *J Chem Ecol,* **27,** 1911-1928.

Whalen, E. D., Grandy, A. S., Sokol, N. W., Keiluweit, M., Ernakovich, J., Smith, R. G.*, et al.* (2022) Clarifying the evidence for microbial-and plant-derived soil organic matter, and the path toward a more quantitative understanding. *Global Change Biology,* **28,** 7167-7185.

Whiteley, M., Diggle, S. P. and Greenberg, E. P. (2017) Progress in and promise of bacterial quorum sensing research. *Nature,* **551,** 313-320.

Williams, A., Langridge, H., Straathof, A. L., Fox, G., Muhammadali, H., Hollywood, K. A.*, et al.* (2021) Comparing root exudate collection techniques: An improved hybrid method. *Soil Biol Biochem,* **161,** 108391.

Yan, S., Yin, L., Dijkstra, F. A., Wang, P. and Cheng, W. (2023) Priming effect on soil carbon decomposition by root exudate surrogates: A meta-analysis. *Soil Biology and Biochemistry,* **178,** 108955.

Yore, M. M., Syed, I., Moraes-Vieira, P. M., Zhang, T., Herman, M. A., Homan, E. A.*, et al.* (2014) Discovery of a class of endogenous mammalian lipids with anti-diabetic and anti-inflammatory effects. *Cell,* **159,** 318-332.

Zhalnina, K., Louie, K. B., Hao, Z., Mansoori, N., da Rocha, U. N., Shi, S.*, et al.* (2018) Dynamic root exudate chemistry and microbial substrate preferences drive patterns in rhizosphere microbial community assembly. *Nature Microbiology,* **3,** 470-480.

Zhang, J., Subramanian, S., Stacey, G. and Yu, O. (2009) Flavones and flavonols play distinct critical roles during nodulation of Medicago truncatula by Sinorhizobium meliloti. *Plant J,* **57,** 171-183.